International Journal of Control, Automation and Systems 19(12) (2021) 3853-3861
http://dx.doi.org/10.1007/s12555-020-0724-y
ISSN:1598-6446 eISSN:2005-4092
http://www.springer.com/12555

Energy Optimization on Wireless-networked Control Systems (W-NCSs) Using Linear Quadratic Gaussian (LQG)

Subchan Subchan, Zuhair Zuhair, Tahiyatul Asfihani, Dieky Adzkiya, and Seungkeun Kim*

Abstract: In a wireless networked control system (W-NCS), energy is required to transmit a sensor reading to the controller. It should be noted that the packet success rate (PSR) is an essential factor in the control performance, and PSR is directly proportional to the energy per symbol. Hence, it requires a significant amount of energy to have perfect control performance. However, in most cases in wireless sensor network scenarios, each node is attached to a limited power battery. Therefore, an energy optimization scheme that can harvest energy while maintaining the control performance is essentially required. The combination of Kalman filter and Linear Quadratic Regulator (LQR) that is known as Linear Quadratic Gaussian (LQG) is used as the backbone of the scheme to estimate the state and synthesize the optimal control. In addition, the optimal power scheduler (PS) is introduced to minimize energy usage while maintaining control performance. The finite block length approach is applied to achieve the upper bound of packet error rate. The results of energy consumption optimization showed that the scheme worked perfectly, wherein the energy per symbol usage is low, and the stability of the dynamic system is well maintained.

Keywords: Energy optimization, LQG control, packet success rate, W-NCSs.

1. INTRODUCTION

Wireless sensor network (WSN) is more commonly implemented rather than the conventional one because of its scalability, accuracy, reliability, low cost, and mobility to construct the concept of the Internet of Things (IoT) [1–5]. A WSN is defined as a system that consists of small tools, named sensor nodes, that operate collaboratively and spread spatially to convey data from the observed plant over wireless channels [3]. In most cases, the wireless sensor node is implemented with a short energy component. Communication is the most significant proportion of energy consumption, especially for transmitting a sensor reading from the plant to the controller.

In W-NCS with a fading channel, there is a possibility that the data from the plant is not successfully delivered to the demodulator/decoder block in the controller. Consequently, the estimator will not receive the quantized signal and fails to estimate the sensor reading. In the closed-loop system, when the controller fails to receive a sensor reading, such a system will be an open loop. Accordingly, the controller fails to generate an updated feedback input signal that can lead to the destabilization of the plant. Therefore, a scheme that can harvest energy while maintaining control performance is needed.

Wireless sensor network optimization by maintaining transmission and reducing power consumption was proposed by Kwon and Jee [6]. Shah *et al*. [7], presented a review of different optimization algorithms to maintain a balance between user comfort and energy requirements, such that the energy consumption is minimized. The optimal expansion planning approach of multiple energy systems based on energy hub was proposed by Zhang *et al*. [8]. Tian *et al*. [9] discussed optimization of multiple energy interconnection networks. Wang *et al*. [10] presented a distributed optimization algorithm by considering a random sleep scheme. Optimal control and stabilization in simultaneous local and remote controller for networked control systems (NCSs) was proposed by Liang *et al*. [11]. Recently, Liang *et al*. [12] studied the optimal control and stabilization in NCSs with asymmetric information. The study of fundamental limitations in the control design and performance of linear time-invariant (LTI) systems have been extensively studied for problems of control over communication networks [13]. It should be noted that signal-to-noise ratio (SNR) can characterize the quality of communication channels. Thus, SNR directly impacts the stability and performance of W-NCSs. The stability anal-

Manuscript received September 29, 2020; revised May 30, 2021; accepted July 7, 2021. Recommended by Associate Editor Le Van Hien under the direction of Editor-in-Chief Keum-Shik Hong. This work was supported by World Class Professor Program 2020 contract number 101.27/E4.3/KU/2020.

Subchan Subchan, Zuhair Zuhair, Tahiyatul Asfihani, and Dieky Adzkiya are with the Department of Mathematics, Institut Teknologi Sepuluh Nopember, Kampus ITS Sukolilo-Surabaya 60111, Indonesia (e-mails: subchan@matematika.its.ac.id, zuhair98zahir@gmail.com, {t_asfihani, dieky}@matematika.its.ac.id). Seungkeun Kim is with the Department of Aerospace Engineering, Chungnam National University, Korea (e-mail: skim78@cnu.ac.kr).
* Corresponding author.

ysis based on SNR has been extensively investigated in [14–16]. Although it would be ideal to have a high SNR that guarantees the successful delivery of the sequence of symbols, a massive amount of energy is required for such a scenario, which is not a perfect choice in limited-energy devices in the long run. LQG control via wireless sensor networks with minimal transmission power is examined in [17,18]. Similar to the research of Balaghiinaloo *et al*. [19], which considered transmission power control and event triggering, Gatsis *et al*. [20] minimized a cost involving the communication energy and the control cost for linear systems. Varma *et al*. [21] minimized the communication energy while guaranteeing a certain linear quadratic performance using time-triggered communication policies for W-NCSs. The characteristics of LQG in wireless sensor networks with minimal transmission power are as follows: an arrival process is involved in the optimal estimation of the system, which shows whether the measurement data is successfully transmitted or not, and separation in the designs of optimal estimator, controller, and transmission power controller is fulfilled.

In this paper, we combine Kalman filter and Linear Quadratic Regulator (LQR), which is defined as Linear Quadratic Gaussian, as the backbone of the scheme to estimate the state and determine the optimal control. This paper presents different representations of the optimal state estimator and controller from the existing work in [17], which (8), (9), (20) are proven by consistent mathematical processes. In addition, the optimal power scheduler (PS) is included in minimizing the energy per symbol usage while keeping the control performance, where the approximation approach is used to ease the computational burden by defining the state estimation at PS. The finite block length approach is applied to achieve the upper bound of a packet error rate. The advantages of using explicit functions of SNR and finite block length approach are the mathematical model becomes closer and more relevant to real systems [22,23]. Throughout this paper, we propose a scheme that minimizes the energy usage on W-NCS over fading channels by using the control performance as a constraint in the optimization problem.

2. MATHEMATICAL MODELS

2.1. Dynamical system model

The plant is attached by a wireless sensor node as a transmitter, which transmits the sensor data through a lossy wireless channel. The block diagram of NCS is shown in Fig. 1. For the k-th time step, the state (x_k) is sent from the plant to the measurement sensor. Then, the output of the system (y_k) is quantized by a high-resolution quantizer into codewords. After that, the signal is encoded to a series of symbols h_k with a specific length before it is sent across a wireless channel. After the controller receives the estimated sensor reading ($\hat{x}_k$) from the estimator, the controller sends the input signal u_k to the plant.

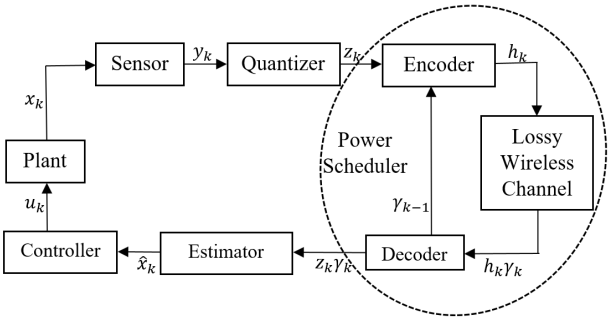

Fig. 1. Block diagram of NCS.

The optimal estimation of state ($\hat{x}_k$) is obtained by Theorem 1, which is required to achieve the optimal controller (u_k) that is formulated by Theorem 3. PS in the plant has to decide the optimal energy per symbol usage by determining the optimal PSR, which is presented in Theorem 4. If the PSR is higher, the energy per symbol is also higher and the possibility that the decoder receives the data successfully is higher as well. It should be noted that when the decoder block fails to receive the sensor reading, the controller may generate updated feedback that may destabilize the system. Therefore, PS has to determine the minimum PSR that maintains the plant stability. The stability is considered by the root-mean-square error (RMSE) between the state of the plant (x) and state reference (x_{ref}). To ease the computation process, the optimal PSR is obtained by using an approximation approach, where the error between estimators at PS ($\check{x}$ in Theorem 2) and controller ($\hat{x}$ in Theorem 1) is involved. Therefore, we assume that the controller can finish all the required steps before the next input arrives.

An explicit discrete-time LTI model of the plant is

$$\begin{aligned} x_k &= Fx_{k-1} + Bu_{k-1} + w_{k-1}, \\ y_k &= Hx_k + v_k, \\ z_k &= y_k + n_k, \end{aligned} \tag{1}$$

where $x_k \in \mathbb{R}^a$ represents the state of the system at time k, $u_k \in \mathbb{R}^b$ is the input signal executed at time k, and $w_k \in \mathbb{R}^a$ is the process noise. The constant matrices $F \in \mathbb{R}^{a\times a}$ and $B \in \mathbb{R}^{a\times b}$ are the state and input matrix, respectively. The system is assumed to be controllable and observable. The measurement of sensor, the output matrix, and the measurement noise of sensor at time k are denoted by $y_k \in \mathbb{R}^c$, $H \in \mathbb{R}^{c\times b}$, and $v_k \in \mathbb{R}^c$, respectively. The process noise w_k, the measurement noise v_k, and the quantizer noise n_k are assumed to be i.i.d with $w_k \sim \mathcal{N}(0,R_1)$, $v_k \sim \mathcal{N}(0,R_2)$, and $n_k \sim \mathcal{N}(0,R_3)$ where $R_1,\ R_2,\ R_3 \succ 0$ denotes the variance of Gaussian distributions.

2.2. Communication channel model

As shown in Fig. 1, the quantized signal z_k is encoded by an encoder as data symbol h_k of length n. It should be considered that the data h_k is transferred via a lossy wireless channel. Hence, there exists a probability that h_k is not received by the decoder. Therefore, the i.i.d. Bernoulli arrival process γ_k is introduced as follows:

$$\gamma_k = \begin{cases} 1, & \text{if } h_k \text{ is transmitted successfully,} \\ 0, & \text{otherwise.} \end{cases} \tag{2}$$

Afterward, the decoder maps h_k back to z_k, the estimator generates estimated signal $\hat{x}_k$ as an input to the controller. The perfect communication channel without noise between the controller and the plant is assumed. Consequently, the controller is constantly able to send an input signal u_k to the plant.

The packet error rate (PER) is specified by $\text{PER}_k = \mathbb{P}\{\gamma_k = 0\}$, where $\mathbb{P}$ is the probability function. The signal-to-noise ratio is symbolized by ρ and formulated as $\rho_k = E_{s_k}/N_0$, where E_{s_k} is the energy per symbol, and N_0 is the noise power spectral density.

The finite block length approach is applied to achieve the upper bound of packet error rate. Therefore, the PER is determined by [23]:

$$\text{PER}_k = 1 - \exp\left(\frac{1 - 2^{\left(\frac{R_c}{B_n} - \frac{\log_2 n}{2n}\right)}}{2\beta^2 \rho_k} \right), \tag{3}$$

where β denotes the scale of Rayleigh distribution, R_c is the communication rate, n is the length of data symbol h_k, and B_n is the noise bandwidth. Since the packet success rate of data transmission is $\text{PSR}_k = 1 - \text{PER}_k$, we can obtain the PSR as the argument of energy per symbol function as

$$E_{s_k} = \begin{cases} \dfrac{m_0}{\ln \text{PSR}_k}, & \text{PSR}_k \in [p,\ q], \\ 0, & \text{PSR}_k = 0, \end{cases} \tag{4}$$

where $[p,\ q]$ is the codomain of PSR_k, and

$$m_0 = \frac{N_0}{2\beta^2} \left(1 - 2^{\left(\frac{R_c}{B_n} - \frac{\log_2 n}{2n}\right)} \right).$$

We denote the function in (4) by $E_{s_k} = \psi(\text{PSR}_k)$ defined in the domain $\mathfrak{S} = 0 \cup [p,\ q]$.

3. METHODS

3.1. Energy optimization model

Suppose that $\mathcal{I}_k = \{\gamma_{0:k-1}, u_{0:k-1}, z_{0:k-1}\}$ is the information provided to the controller at time k. We also define the information available to PS at time k as $\mathcal{I}_k^s = \{\gamma_{0:k-1}, u_{0:k-1}, z_{0:k}\}$. Therefore, $\mathcal{I}_k \subseteq \mathcal{I}_k^s$. The objective function of this scheme is minimizing

$$J = \mathbb{E}\left[\sum_{k=0}^{N} \psi(\text{PSR}_k) \right], \tag{5}$$

subject to

$$\mathbb{E}\left[\|x_{N+1}\|_{Q_0}^2 + \sum_{k=0}^{N} \left(\|x_k\|_{Q_1}^2 + \|u_k\|_{Q_2}^2 \right) \right] \leq \theta, \tag{6}$$

where θ is the level of control performance, N is the time horizon, and the weighting matrices Q_0, $Q_1 \succeq 0$ and $Q_2 \succ 0$ [17]. Since $E_{s_k} = \psi(\text{PSR}_k)$, it should be noted that objective function in (5) is equal to the average of energy per symbol usage over the time horizon. Let PSR^* and u^* be the optimal PSR and control, respectively. By using (5) and (6), we obtain

$$\mathcal{H} = \inf_{\text{PSR}^*, u^*} \mathbb{E}\left[\lambda \|x_{N+1}\|_{Q_0}^2 + \sum_{k=0}^{N} \left(\psi(\text{PSR}_k) + \lambda \|x_k\|_{Q_1}^2 + \lambda \|u_k\|_{Q_2}^2 \right) \right], \tag{7}$$

where $\lambda > 0$ is a weighting constant. In this work, the optimum PSR^* and u^* that keep the stability of the dynamic system with low energy usage will be determined.

3.2. Optimal estimator

In this subsection, we design optimal estimators at the controller and power scheduler (PS). The optimal estimation of the state is based on Kalman Filter [24] and a modification of the optimal estimator representation in [17] with consistent mathematical proof. The optimal estimation is necessary to obtain the optimal control, which will be discussed in Subsection 3.3.

Theorem 1: Optimal estimation of the system state (1) through a lossy wireless channel with arrival process (2) is obtained by minimizing the mean square error (MSE)

$$\hat{x}_{k+1} = F\hat{x}_k + Bu_k + \gamma_k F K_k (z_k - H\hat{x}_k), \tag{8}$$

$$P_{k+1} = F P_k F^T + R_1 - \gamma_k F K_k H P_k F^T, \tag{9}$$

where $\hat{x}_k = \mathbb{E}[x_k | \mathcal{I}_k]$, $P_k = \text{Var}[x_k | \mathcal{I}_k]$, and $K_k = P_k H^T \left(H P_k H^T + \bar{R}_2 \right)^{-1}$, with initial condition $\hat{x}_0 = m_0$, $P_0 = R_0$, and $\bar{R}_2 = R_2 + \Lambda$.

Proof: We determine the a-priori estimated state at time $k+1$ as $\hat{x}_{k+1} = \mathbb{E}[x_{k+1} | \mathcal{I}_{k+1}]$, while the a-posteriori estimated state at time k as $\hat{x}_{k^+} = \mathbb{E}[x_k | \mathcal{I}_{k+1}]$. Therefore, by using (1) we obtain

$$\hat{x}_{k+1} = F\hat{x}_{k^+} + Bu_k. \tag{10}$$

Furthermore, the a-priori error covariance at time $k+1$ and the a-posteriori error covariance at time k are formulated by $P_{k+1} = \mathrm{Var}\left[x_{k+1} - \hat{x}_{k+1} | \mathcal{I}_{k+1}\right]$ and $P_{k^+} = \mathrm{Var}[(x_k - \hat{x}_{k^+}) | \mathcal{I}_k]$, respectively. Thus, by using (1) and (10) we obtain

$$P_{k+1} = F P_{k^+} F^T + R_1. \tag{11}$$

The innovation of measurements is denoted by $\tilde{z}_k = z_k - \hat{z}_k$ where $\hat{z} = \mathbb{E}[z_k]$ is the estimated measurement. Then, the a-posteriori estimated state is specified by $\hat{x}_{k^+} = \hat{x}_k + \gamma_k K_k \tilde{z}_k$, where K_k is the Kalman gain. We define $\bar{R}_2 = R_2 + \Lambda$, and write the a-posteriori error covariance at time k as $P_{k^+} = P_k - \gamma_k K_k H P_k - \gamma_k P_k H^T K_k^T + \gamma_k K_k \left(H P_k H^T + \bar{R}_2\right) K_k^T$. In order to get the minimum value of mean square error of the estimated state, we find K_k such that $\mathrm{tr}(P_{k+1})$ in (11) is minimum. Hence, we take the derivative of trace of P_{k^+} with respect to K_k equal to zero. We obtain $K_k = P_k H^T \left(H P_k H^T + \bar{R}_2\right)^{-1}$, and

$$P_{k^+} = \left(I_n - \gamma_k P_k H^T \left(H P_k H^T + \bar{R}_2\right)^{-1} H\right) P_k, \tag{12}$$

$$\hat{x}_{k^+} = \hat{x}_k + \gamma_k P_k H^T \left(H P_k H^T + \bar{R}_2\right)^{-1} (z_k - H\hat{x}_k). \tag{13}$$

We obtain the result by substituting (12) and (13) in (11) and (10), respectively. □

The approximation approach is applied to ease the computing cost of dynamic programming that is used in the optimal power scheduler to determine the optimal PSR, which will be discussed in Subsection 3.4. The approximation approach is employed by calculating errors between the estimators at PS and the controller. Therefore, optimal estimation of the state at PS is designed.

Theorem 2: The optimal estimated state at PS for $0 \leq k < N$ satisfies:

$$\check{x}_{k+1} = F\check{x}_k + Bu_k + K_k^s \left(z_k - H\left(F\check{x}_k + Bu_k\right)\right), \tag{14}$$

$$P_{k+1}^s = \left(\left(F P_k^s F^T + R_0\right)^{-1} + H^T R_2^{-1} H\right)^{-1}, \tag{15}$$

$$K_k^s = P_k^s H^T R_2^{-1}, \tag{16}$$

with initial condition, $\check{x}_0 = m + P_0^s H^T \bar{R}_2^{-1}(z_0 - Hm)$, $m = \mathbb{E}[x_0]$, $P_0^s = \left(R_0^{-1} + H^T \bar{R}_2 H\right)^{-1}$, where $\check{x}_k = \mathbb{E}\left[\check{x}_k | \mathcal{I}_k^s\right]$, and $P_k^s = \mathrm{Var}\left[\check{x}_k | \mathcal{I}_k^s\right]$.

Proof: Similar proof to Theorem 1. □

3.3. Optimal control

The basic scheme of optimal control is based on [25] and modification of [17] with consistency in mathematical proof. On the basis of [25], the cost function in (7) can be written as

$$\mathcal{H} = \inf \mathbb{E}\left[\sum_{k=0}^{t-1} \left(\psi(\mathrm{PSR}_k) + \lambda \|x_k\|_{Q_1}^2 + \lambda \|u_k\|_{Q_2}^2\right)\right.$$
$$\left. + \mathbb{E}\left[\lambda \|x_{N+1}\|_{Q_0}^2 + \sum_{k=t}^{N} \left(\psi(\mathrm{PSR}_k) + \lambda \|x_k\|_{Q_1}^2 + \lambda \|u_k\|_{Q_2}^2\right)\right]\right], \tag{17}$$

with certain u^* and PSR^*. It is clear that the first term in (17) is independent of $u(t), u(t+1), \ldots, u(N)$. Thus, by assuming there is a unique minimum value, we define a value function

$$V_k = \min_{\mathrm{PSR}^*, u^*} \mathbb{E}\left[\|x_{N+1}\|_{Q_0}^2 + \sum_{t=k}^{N} \left(\frac{1}{\lambda}\psi(\mathrm{PSR}_t) + \|x_t\|_{Q_1}^2 + \|u_t\|_{Q_2}^2\right) | \mathcal{I}_k\right]. \tag{18}$$

Therefore, the cost function in (7) is represented by $\Psi(\mathrm{PSR}^*, u^*) = \lambda \mathbb{E}[V_0]$.

Theorem 3: The optimal control is $u_k^* = -L_k \hat{x}_k$ where

$$L_k = \left(Q_2 + B^T S_{k+1} B\right)^{-1} B^T S_{k+1} F, \tag{19}$$

where $S \succeq 0$ is the solution of Riccati equation

$$S_k = F^T S_{k+1} + Q_1 - L_k^T \left(B^T S_{k+1} B + Q_2\right) L_k, \tag{20}$$

with $S_{N+1} = Q_0$.

Proof: To make sure that there is one minimum value of V_k for each k, we prove by backward induction that the value function satisfies the convex form $V_k = \hat{x}_k^T S \hat{x}_{k+1} + s_k$ where $S_k \succ 0$ and s_k is independent of x_k and $\hat{x}_k$. The case is assumed to be true for time $k+1$, and we would like to prove that it is also true for time k. By using the claim and properties of expected value, we can rewrite the value function as

$$V_k = \min_{\mathrm{PSR}_k, u_k} \left\{\frac{1}{\lambda}\psi(\mathrm{PSR}_k) + \mathbb{E}\left[x_k^T Q_1 x_k | \mathcal{I}_k\right] + u_k^T Q_2 u_k \right.$$
$$\left. + \mathbb{E}\left[\hat{x}_{k+1}^T S_{k+1} \hat{x}_{k+1} | \mathcal{I}_k\right] + \mathbb{E}\left[s_{k+1} | \mathcal{I}_k\right]\right\}. \tag{21}$$

We know that $\mathbb{E}\left[\tilde{z}_k \tilde{z}_k^T | \mathcal{I}_k\right] = H P_k H^T + \bar{R}_2$ by the fact that $P_k = \mathrm{Var}\left[x_k | \mathcal{I}_k\right]$. Therefore, by applying the properties of covariance and using (8) we obtain $\mathrm{Var}\left[\hat{x}_{k+1} | \mathcal{I}_k\right] = \mathrm{PSR}_k F K_k \left(H P_k H^T + \bar{R}_2\right) K_k^T F^T$. Thus, we can get

$$\mathbb{E}\left[\hat{x}_{k+1}^T S_{k+1} \hat{x}_{k+1} | \mathcal{I}_k\right]$$
$$= \left(F\hat{x}_k + Bu_k\right)^T S_{k+1} \left(F\hat{x}_k + Bu_k\right)$$
$$+ \mathrm{PSR}_k \mathrm{tr}\left(S_{k+1} F K_k \left(H P_k H^T + \bar{R}_2\right) K_k^T F^T\right). \tag{22}$$

Since $\mathbb{E}\left[x_k^T Q_1 x_k | \mathcal{I}_k\right] = \hat{x}_k^T Q_1 \hat{x}_k + \mathrm{tr}(Q_1 P_k)$, by substituting (22) in (21) we obtain

$$V_k = \min_{\mathrm{PSR}_k, u_k} \left\{\frac{1}{\lambda}\psi(\mathrm{PSR}_k) + \hat{x}_k^T Q_1 \hat{x}_k + \mathrm{tr}(Q_1 P_k) \right.$$
$$+ u_k^T Q_2 u_k + \left(F\hat{x}_k + Bu_k\right)^T S_{k+1} \left(F\hat{x}_k + Bu_k\right)$$
$$+ \mathrm{PSR}_k \mathrm{tr}\left(S_{k+1} F K_k \left(H P_k H^T + \bar{R}_2\right) K_k^T F^T\right)$$
$$\left. + \mathbb{E}\left[s_{k+1} | \mathcal{I}_k\right]\right\}. \tag{23}$$

Since V_k is a matrix of size 1×1, V_k is equivalent to $\mathrm{tr}(V_k)$. Therefore, to obtain the optimal input u_k we take the derivative of $\mathrm{tr}(V_k)$ with respect to u_k equal to zero. We get $u_k^* = -\left(Q_2+B^TS_{k+1}B\right)^{-1}B^TS_{k+1}F\hat{x}_k$. We define $L_k = \left(Q_2+B^TS_{k+1}B\right)^{-1}B^TS_{k+1}F$, such that $u_k^* = -L_k\hat{x}_k$. Substituting u_k^* and PSR_k^* in (23), we attain

$$\begin{aligned}V_k =&\hat{x}_k^T\left(F^TS_{k+1}F+Q_1-L_k^T\left(B^TS_{k+1}B+Q_2\right)L_k\right)\hat{x}_k\\&+\frac{1}{\lambda}\psi\left(\mathrm{PSR}_k^*\right)+\mathrm{tr}\left(Q_1P_k\right)\\&+\mathrm{PSR}_k^*\,\mathrm{tr}\left(S_{k+1}FK_k\left(HP_kH^T+\bar{R}_2\right)K_k^TF^T\right)\\&+\mathbb{E}\left[s_{k+1}|\mathcal{I}_k\right].\end{aligned}\tag{24}$$

From (24) we can see that the form of $V_k = \hat{x}_k^TS_k\hat{x}_{k+1}+s_k$ is satisfied, where $S_k = F^TS_{k+1}F+Q_1-L_k^T(B^TS_{k+1}B+Q_2)L_k$, and $s_k = \frac{1}{\lambda}\psi(\mathrm{PSR}_k^*)+\mathrm{tr}(Q_1P_k)+\mathrm{PSR}_k^*\,\mathrm{tr}(S_{k+1}FK_k(HP_kH^T+\bar{R}_2)K_k^TF^T)+\mathbb{E}[s_{k+1}\mid\mathcal{I}_k]$. □

3.4. Optimal packet success rate

In this subsection, we determine the optimal PSR in Theorem 4. We apply discussed theorems and construct the following lemma to ease the formulation of optimal PSR.

Lemma 1: The cost function $\Psi(\mathrm{PSR},u^*)$ with optimal control u^* from Theorem 3 and PSR which are independent to x and $\hat{x}$ is

$$\begin{aligned}&\Psi\left(\mathrm{PSR},u^*\right)\\&=\lambda m^TS_0m+\mathbb{E}\Bigg[\sum_{k=0}^{N}\psi(\mathrm{PSR}_k)+\lambda w_k^TS_{k+1}w_k\\&\quad+\lambda\left(u_k+L_kx_k\right)^T\left(B^TS_{k+1}B+Q_2\right)\left(u_k+L_kx_k\right)\Bigg].\end{aligned}\tag{25}$$

Proof: Using the process dynamics (1) and the Riccati equation (20), we can write

$$\begin{aligned}&x_{k+1}^TS_{k+1}x_{k+1}\\&=\left(Fx_k+Bx_k+w_k\right)^TS_{k+1}\left(Fx_k+Bx_k+w_k\right),\end{aligned}\tag{26}$$

$$\begin{aligned}&x_k^TS_kx_k\\&=x_k^T\left(F^TS_{k+1}F+Q_1-L_k^T\left(B^TS_{k+1}B+Q_2\right)L_k\right)x_k.\end{aligned}\tag{27}$$

Subsequently, we obtain

$$\begin{aligned}&x_{N+1}^TS_{N+1}x_{N+1}-x_0^TS_0x_0\\&=\sum_{k=0}^{N}\Big\{w_k^TS_{k+1}w_k+2\left(Fx_k+Bu_k\right)^TS_{k+1}w_k\\&\quad+x_k^TL_k^T\left(B_k^TS_{k+1}B_k+Q_2\right)L_kx_k\\&\quad-x_k^TQ_1x_k-u_k^TQ_2u_k+2x_k^TF_k^TS_{k+1}B_ku_k\\&\quad+u_k^T\left(B_k^TS_{k+1}B_k+Q_2\right)u_k\Big\},\end{aligned}$$

where we used (26) and (27). By applying some algebraic operations, we obtain

$$\begin{aligned}&\Psi\left(\mathrm{PSR},u^*\right)\\&=\mathbb{E}\Bigg[\lambda x_0^TS_0x_0+\sum_{k=0}^{N}\Big\{\psi(\mathrm{PSR}_k)+\lambda w_k^TS_{k+1}w_k\\&\quad+2\lambda\left(Fx_k+Bu_k\right)^TS_{k+1}w_k\\&\quad+\lambda\left(u_k+L_kx_k\right)^T\left(B_k^TS_{k+1}B_k+Q_2\right)\left(u_k+L_kx_k\right)\Big\}\Bigg]\\&=\lambda m^TS_0m+\mathbb{E}\Bigg[\sum_{k=0}^{N}\psi(\mathrm{PSR}_k)+\lambda w_k^TS_{k+1}w_k\\&\quad+\lambda\left(u_k+L_kx_k\right)^T\left(B^TS_{k+1}B+Q_2\right)\left(u_k+L_kx_k\right)\Bigg],\end{aligned}$$

where in the second equality we used the fact that w_k is independent of x_k. □

Suppose that $e_k = x_k-\hat{x}_k$ is the estimation error, and $\varepsilon_k = \check{x}_k-\hat{x}_k$ is the error between estimators at the PS and the controller, where $\hat{x}_k$ is obtained from (8) in Theorem 1, and $\check{x}_k$ is obtained from (14) in Theorem 2.

Theorem 4: The optimal packet success rate is

$$\begin{aligned}&\mathrm{PSR}_k^*\\&=\underset{\mathrm{PSR}_k\in\mathfrak{S}}{\mathrm{argmin}}\Big\{\psi\left(\mathrm{PSR}_k\right)+\mathrm{PSR}_k\,\tilde{z}^TK_k^TF^T\\&\quad L_{k+1}^T(B^TS_{k+2}B+Q_2)L_{k+1}F\left(K_k\tilde{z}-2\varepsilon_k\right)+\hat{\rho}_k\Big\},\end{aligned}\tag{28}$$

where $\hat{\rho}_k = \mathbb{E}\left[V_{k+1}^s|\mathcal{I}_k^s\right]$,

$$V_k^s = \min_{\mathrm{PSR}_k}\mathbb{E}\left[\sum_{t=k}^{N}\psi(\mathrm{PSR}_t)+\lambda e_{t+1}^T\Gamma_{t+1}e_{t+1}\middle|\mathcal{I}_k^s\right],$$

and $\Gamma_k = L_k^T(B^TS_{k+1}B+Q_2)L_k$ with the exception of $\Gamma_{N+1}=0$.

Proof: Applying Lemma 1, we acquire

$$\begin{aligned}\Psi\left(\mathrm{PSR},u^*\right)=&\lambda m^TS_0m\\&+\mathbb{E}\Bigg[\sum_{k=0}^{N}\psi(\mathrm{PSR}_k)+\lambda w_k^TS_{k+1}w_k\\&+\lambda e_k^TL_k^T(B^TS_{k+1}B+Q_2)L_ke_k\Bigg].\end{aligned}$$

We specify the value function V_k^s as $V_k^s = \min_{\mathrm{PSR}_k}\mathbb{E}\left[\sum_{t=k}^{N}\psi(\mathrm{PSR}_t)+\lambda e_{t+1}^T\Gamma_{t+1}e_{t+1}\middle|\mathcal{I}_k^s\right]$, where $\Gamma_k = L_k^T(B^TS_{k+1}B+Q_2)L_k$ with the exception of $\Gamma_{N+1}=0$. We obtain

$$V_k^s = \min_{\mathrm{PSR}_k}\mathbb{E}\left[\psi(\mathrm{PSR}_k)+\lambda e_{k+1}^T\Gamma_{k+1}e_{k+1}+V_{k+1}^s\middle|\mathcal{I}_k^s\right],$$

where the additivity property is implemented, and $V_{N+1}^s = 0$. It is obvious that V_k^s does not depend on u_k for time $N+1$. We claim that it is satisfied for time $k+1$ as in the hypothesis of backward induction, and we will show that it is also satisfied for time k. Let the dynamics of the estimation error at the controller be $e_{k+1} = Fe_k + w_k - \gamma_k K_k \tilde{z}_k$. Thus, we find

$$\begin{aligned}
&\mathbb{E}\left[e_{k+1}^T \Gamma_{k+1} e_{k+1} \middle| \mathcal{I}_k^s\right] \\
&= \varepsilon_k^T F^T \Gamma_{k+1} F \varepsilon_k + \operatorname{tr}(F^T \Gamma_{k+1} F P_k^s) + \operatorname{tr}(\Gamma_{k+1} W_k) \\
&\quad + \mathrm{PSR}_k \tilde{z}_k^T K_k^T F^T \Gamma_{k+1} F K_k \tilde{z}_k \\
&\quad - 2\,\mathrm{PSR}_k \tilde{z}_k^T K_k^T F^T \Gamma_{k+1} F \varepsilon_k.
\end{aligned}$$

Therefore, we get

$$\begin{aligned}
V_k^s &= \min_{\mathrm{PSR}_k} \left\{ \psi(\mathrm{PSR}_k) + \lambda\, \mathbb{E}\left[e_{k+1}^T \Gamma_{k+1} e_{k+1} \middle| \mathcal{I}_k^s\right] \right. \\
&\quad \left. + \mathbb{E}\left[V_{k+1}^s \middle| \mathcal{I}_k^s\right] \right\} \\
&= \min_{\mathrm{PSR}_k} \left\{ \psi(\mathrm{PSR}_k) + \lambda \varepsilon_k^T F^T \Gamma_{k+1} F \varepsilon_k \right. \\
&\quad + \operatorname{tr}(F^T \Gamma_{k+1} F P_k^s) + \operatorname{tr}(\Gamma_{k+1} W_k) \\
&\quad + \mathrm{PSR}_k \tilde{z}_k^T K_k^T F^T \Gamma_{k+1} F K_k \tilde{z}_k \\
&\quad \left. - 2\,\mathrm{PSR}_k \tilde{z}_k^T K_k^T F^T \Gamma_{k+1} F \varepsilon_k + \mathbb{E}\left[V_{k+1}^s \middle| \mathcal{I}_k^s\right] \right\}.
\end{aligned} \tag{29}$$

The minimizer in (29) is found as

$$\begin{aligned}
\mathrm{PSR}_k^* = \operatorname*{argmin}_{\mathrm{PSR}_k \in \mathfrak{S}} \big\{ & \psi(\mathrm{PSR}_k) \\
& + \mathrm{PSR}_k \tilde{z}^T K_k^T F^T \Gamma_{k+1} F (K_k \tilde{z} - 2\varepsilon_k) + \hat{\rho}_k \big\},
\end{aligned}$$

where $\hat{\rho}_k = \mathbb{E}\left[V_{k+1}^s | \mathcal{I}_k^s\right]$. From the hypothesis assumption, $\hat{\rho}_k$ is independent of the control policy. □

4. RESULTS AND DISCUSSIONS

A wheeled inverted pendulum is used as the plant because of its instability and simplicity that is sufficient to represent the common necessity of a control system in W-NCS. The input of system is the controlled horizontal force which is applied to the cart, and the outputs are the deviation angle of the pendulum from the equilibrium (ϕ) and the horizontal position of the plant (μ). We denote the system state as $x(t) = \begin{bmatrix}\mu(t) & \dot{\mu}(t) & \phi(t) & \dot{\phi}(t)\end{bmatrix}^T$ with the equations of motion of the system that is linearized around the vertical upward equilibrium position of the pendulum as [26]

$$\begin{aligned}
\dot{x}(t) = &\begin{bmatrix} 0 & 1 & 0 & 0 \\ 0 & \frac{-(I+\mathfrak{m}l^2)\mathfrak{b}}{\mathfrak{I}(M+\mathfrak{m})+M\mathfrak{m}l^2} & \frac{\mathfrak{m}^2 g l^2}{\mathfrak{I}(M+\mathfrak{m})+M\mathfrak{m}l^2} & 0 \\ 0 & 0 & 0 & 1 \\ 0 & \frac{-\mathfrak{m}l\mathfrak{b}}{\mathfrak{I}(M+\mathfrak{m})+M\mathfrak{m}l^2} & \frac{\mathfrak{m}gl(M+\mathfrak{m})}{\mathfrak{I}(M+\mathfrak{m})+M\mathfrak{m}l^2} & 0 \end{bmatrix} x(t) \\
&+ \begin{bmatrix} 0 \\ \frac{\mathfrak{I}+\mathfrak{m}l^2}{\mathfrak{I}(M+\mathfrak{m})+M\mathfrak{m}l^2} \\ 0 \\ \frac{\mathfrak{m}l}{\mathfrak{I}(M+\mathfrak{m})+M\mathfrak{m}l^2} \end{bmatrix} u(t) + w(t), \\
y(t) = &\begin{bmatrix} 1 & 0 & 0 & 0 \\ 0 & 0 & 1 & 0 \end{bmatrix} x(t) + v(t),
\end{aligned} \tag{30}$$

where mass of the pendulum ($\mathfrak{m}$) = 0.2 kg, mass of the cart (M) = 0.5 kg, the length to pendulum center of mass (l) = 0.3 m, mass moment of inertia of the pendulum ($\mathfrak{I}$) = 0.006 kg m^2, the coefficient of gravity (g) = 9.8 m/s^2, the coefficient of friction for wheels ($\mathfrak{b}$) = 0.1 N/m/s. A zero order hold (ZOH) is applied for discretizing (30) with sampling time $T_s = 0.01$. The system is simulated over the horizon $N = 1000$, the initial state $x_0 = \begin{bmatrix}0 & 0 & 0.0873 & 0\end{bmatrix}^T$, the mean of x_0 is $m = \begin{bmatrix}0 & 0 & 0 & 0\end{bmatrix}^T$, the reference of the state is $x_{ref} = \begin{bmatrix}1 & 0 & 0 & 0\end{bmatrix}^T$, $R_0 = 2I_4$, $R_1 = 0.0001I_4$, $\bar{R}_2 = 0.0003I_2$, $Q_0 = Q_1 = 100I_3$, where I_n denotes $n \times n$ identity matrix, $Q_2 = 0.5$, and the weighting constant $\lambda = 0.0004$. We use communication parameters $R_c = 1$, $B_n = 1$, $\beta = 1$, $p = 1 \times 10^{-5}$, $q = 1 - 1 \times 10^{-5}$ and the length of data symbol $n = 100$.

In this comparative simulation, the importance of transmission energy optimization will be shown. Since energy is the function of PSR, cases that do not consider energy minimization are represented by determining relatively high-constant PSR and low-constant PSR. Figs. 2-5 show four states of wheeled inverted pendulum and their reference on three different PSR scenarios; optimal PSR (PSR* in Fig. 6, with the average value of 0.5761), high-constant PSR (PSR = 0.8), and low-constant PSR (PSR = 0.01). By looking at Table 1, it is noticeable that the optimal-PSR scenario gives positive impacts on the dynamic of the systems. Compared to the high-constant-PSR scenario (constant $E_{s_k} = J = 2.0390$), the optimal-PSR scenario has considerably lower energy consumption ($\bar{E}_{s_k}^* = J^* = 1.3622$, with the variance of 11.6835, Fig. 7) and still maintains the stability of the system (Figs. 2-5), which is proved by insignificant difference of RMSE of the states between these two scenarios. The first row of

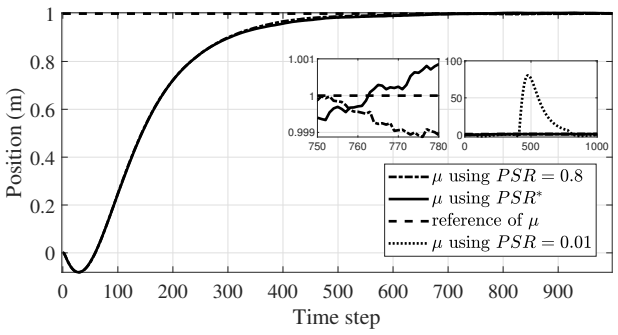

Fig. 2. The horizontal position of the cart.

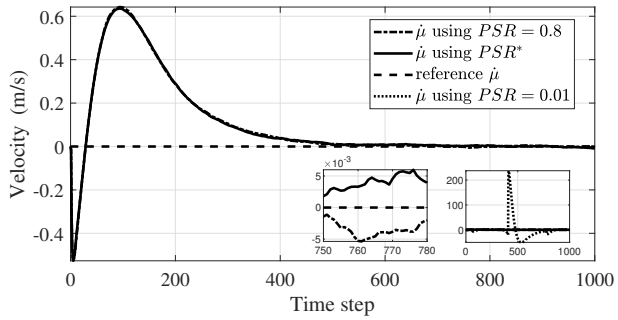

Fig. 3. The velocity of the cart.

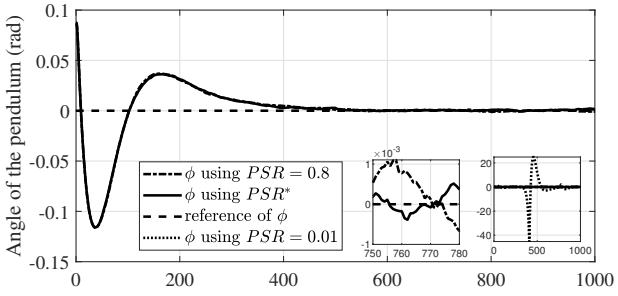

Fig. 4. The deviation angle of the pendulum.

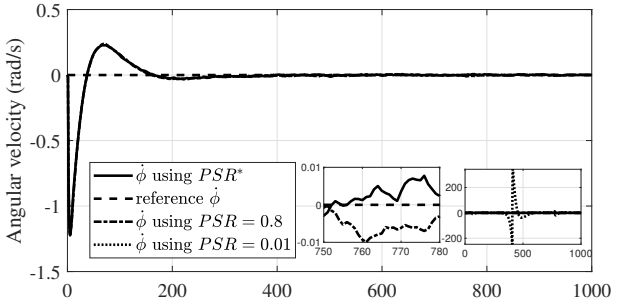

Fig. 5. The angular velocity of the pendulum.

Table 1. The effects of varying the PSR on dynamic of the system.

PSR	RMSE of				Average of	
	μ	$\dot{\mu}$	ϕ	$\dot{\phi}$	$E_{s_k}(J)$	u_k^*
0.01	26.612	40.7288	7.9041	47.6397	0.0988	0.0225
PSR*	0.3564	0.2191	0.0271	0.1394	1.3622	0.0093
0.8	0.3560	0.2203	0.0271	0.1406	2.0390	0.0101

Table 1 depicts that the low-constant PSR scenario fails to reach stability, which has the highest RMSE and the lowest energy consumption (constant $E_{s_k} = J = 0.0988$). Even though the low-constant PSR scenario gives the smallest value of J, it produces instability of the system. From Figs. 6-7, it can be noted that the optimal PSR scenario makes the energy per symbol adaptively change as low as possible while maintaining the stability of the dynamic system. From Table 1, in comparison of energy usage of

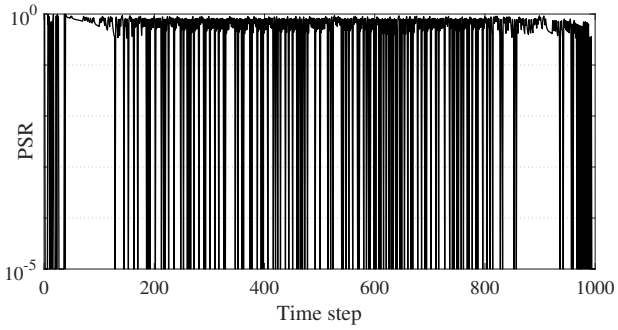

Fig. 6. Optimal packet success rate (PSR*).

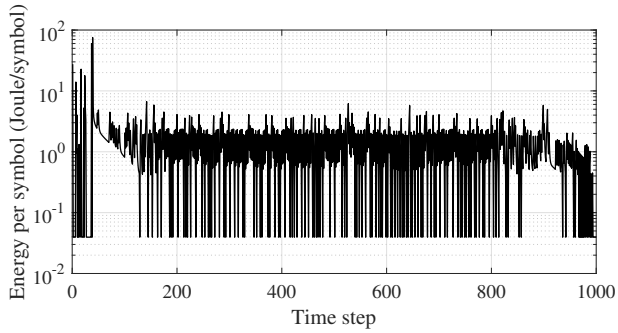

Fig. 7. Energy per symbol using PSR*.

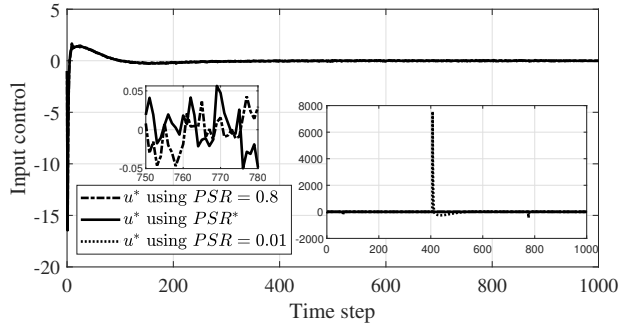

Fig. 8. Optimal control.

two PSR scenarios with similar RMSE values, the scenario with optimal PSR (PSR*) uses 33.19% lower energy than the scenario with high-constant PSR (PSR $= 0.8$). From the average of u_k^* in Table 1 and Fig. 8, it is clear that using the optimal-PSR scenario gives a similar control effort to the high-constant PSR scenario and successfully attains the stability of the system, whereas the low-constant PSR scenario uses the highest control effort but fails to reach stability.

In the case of varying the value of the weighting constant (Table 2), the following facts are observed. As the value of λ becomes larger than 0.0004, the average energy needed increases but there is no significant decrease of RMSE of all states of the system. In contrast, as the value of λ becomes smaller than 0.0004, the average energy

Table 2. The effects of varying λ on dynamic of the system.

λ	Average E_{s_k}	RMSE of μ	RMSE of $\dot{\mu}$	RMSE of ϕ	RMSE of $\dot{\phi}$
4×10^{-7}	0.2250	4.4900	6.9440	1.3418	8.0877
4×10^{-6}	0.3552	6.4577	9.8495	1.9125	11.5246
0.00004	0.9817	0.3584	0.4652	0.5152	2.4166
0.0004	1.4795	0.3567	0.2202	0.0271	0.1387
0.004	4.4282	0.3565	0.2211	0.0272	0.1399
0.04	9.5873	0.3562	0.2203	0.0273	0.1401
0.4	29.6095	0.3561	0.2211	0.0274	0.1404
4	90.4485	0.3554	0.2203	0.0272	0.1395

needed decreases but RMSE of all states starts to increase significantly. Therefore, in this paper, we use $\lambda = 0.0004$.

5. CONCLUSIONS

This paper successfully combines LQR and Kalman Filter that use minimal energy usage on W-NCS while maintaining the stability of the system. The dynamic system reaches stability with the minimum usage of energy. When the weighting constant becomes smaller, the average energy needed decreases, but the system is still stable until $\lambda = 0.0004$.

Overall, the proposed method can be extended to multiple systems or communication channel models with delay or memory. Future research includes also an event-triggered control scheme.

REFERENCES

[1] G. Kortuem, F. Kawsar, V. Sundramoorthy, and D. Fitton, "Smart objects as building blocks for the internet of things," *IEEE Internet Computing*, vol. 14, no. 1, pp. 44-51, 2010.

[2] M. Zorzi, A. Gluhak, S. Lange, and A. Bassi, "From today's intranet of things to a future internet of things: a wireless- and mobility-related view," *IEEE Wireless Communications*, vol. 7, no. 6, pp. 44-51, 2010.

[3] P. Rawat, K. D. Singh, H. Chaouchi, and J. M. Bonnin, "Wireless sensor networks: a survey on recent developments and potential synergies," *Springer Science+Business Media*, vol. 68, pp. 1-48, 2013.

[4] P. Park, S. Coleri Ergen, C. Fischione, C. Lu, and K. H. Johansson, "Wireless network design for control systems: A survey," *IEEE Communications Surveys Tutorials*, vol. 20, no. 2, pp. 978-1013, 2018.

[5] J. P. Hespanha, P. Naghshtabrizi, and Y. Xu, "A survey of recent results in networked control systems," *Proceedings of the IEEE*, vol. 95, no. 1, pp. 138-162, 2007.

[6] Y. Kwon and J. Lee, "Energy optimization model with variable keep-alive cycle algorithm in wireless sensor network," *International Journal of Control, Automation and Systems* , vol. 17, no. 10, pp. 2531-2540, 2019.

[7] A. Shah, H. Nasir, M. Fayaz, A. Lajis, and A. Shah, " A review on energy consumption optimization techniques in IoT based smart building environments," *Information*, vol. 10, no. 3, pp. 108, January 2019.

[8] X. Zhang, M. Shahidehpour, A. Alabdulwahab, and A. Abusorrah, A, "Optimal expansion planning of energy hub with multiple energy infrastructures," *IEEE Transactions on Smart Grid*, vol. 6, no. 5, pp. 2302-2311, 2015.

[9] Y. Tian, Z. Yu, N. Zhao, Y. Zhu, and R. Xia, "Optimized operation of multiple energy interconnection network based on energy utilization rate and global energy consumption ratio," *Proc. of 2nd IEEE Conference on Energy Internet and Energy System Integration (EI2)*, 2018.

[10] Z. Wang, L. Zheng, and H. Li, "Distributed optimization over general directed networks with random sleep scheme," *International Journal of Control, Automation and Systems*, vol. 18 no. 10, pp. 2534-2542, 2020.

[11] X. Liang and J. Xu, "Control for networked control systems with remote and local controllers over unreliable communication channel," *Automatica*, vol. 98, pp. 86-94, 2018.

[12] X. Liang and J. Xu, "Optimal control and stabilization for networked control systems with asymmetric information," *IEEE Transactions on Control of Network Systems*, vol. 7, no. 3, pp. 1355-1365, 2020.

[13] H. Shen, F. Li, S. Xu, and V. Sreeram, "Slow state variables feedback stabilization for semi-Markov jump systems with singular perturbations," *IEEE Transactions on Automatic Control*, vol. 63, no. 8, pp. 2709-2714, Aug 2018.

[14] X.-W. Jiang, B. Hu, Z.-H. Guan, X.-H. Zhang, and L. Yu, "The minimal signal-to-noise ratio required for stability of control systems over a noisy channel in the presence of packet dropouts," *Information Sciences*, vol. 372, pp. 579-590, 2016.

[15] A. J. Rojas and H. O. Garcés, "Signal-to-noise ratio constrained feedback control: discrete-time robust stability analysis," *IET Control Theory & Applications*, vol. 13, no. 3, pp. 444-450, 2018.

[16] A. J. Rojas, "Signal-to-noise ratio constrained feedback control: Robust stability analysis," *ISA Transactions*, vol. 95, pp. 235-242, 2019.

[17] T. Soleymani, S. Hirche, and J. S. Baras, "LQG control via wireless sensor networks with minimal transmission power," *IFAC PapersOnLine*, vol. 51, no. 7, pp. 51-56, 2018.

[18] T. Soleymani, S. Hirche, and J. S. Baras, "Value of Information in Minimum-Rate LQG Control," *IFAC-PapersOnLine*, vol. 50, no. 1, pp. 8963-8968, 2017.

[19] M. Balaghiinaloo, D. Antunes, V. S. Varma, R. Postoyan and W. P. M. H. Heemels, "LQ-power consistent control: Leveraging transmission power selection in control systems," *Proc. of European Control Conference (ECC)*, Saint Petersburg, Russia, 2020.

[20] K. Gatsis, A. Ribeiro, and G. J. Pappas, "Optimal power management in wireless control systems," *IEEE Transactions on Automatic Control*, vol. 59, no. 6, pp. 1495-1510, 2014.

[21] V. S. Varma, A. M. Oliveira, R. Postoyan, I.-C. Morarescu, and J. Daafouz, "Energy-efficient communication policies for wireless networked control systems," *IEEE Transactions on Automatic Control*, vol. 65, no. 10, pp. 4324-4331, 2020.

[22] G. Durisi, T. Koch, and P. Popovski, "Toward massive, ultra reliable, and low-latency wireless communication with short packets," *Proceedings of the IEEE*, vol. 104, no. 9, pp. 1711-1726, 2016.

[23] W. Yang, G. Durisi, T. Koch, and Y. Polyanskiy, "Quasi-static multiple-antenna fading channels at finite block length," *IEEE Transactions on Information Theory*, vol. 60, no. 7, pp. 4232-4265, 2014.

[24] R. E. Kalman, "A new approach to linear filtering and prediction problems," *Transactions of the ASME-Journal of Basic Engineering*, vol. 82 (Series D), pp. 35-45, 1960.

[25] K. J. Astrom, *Introduction to Stochastic Control Theory*, Academic Press, Lund, 1970.

[26] H. Fang and Z. Lin, *An Anti-windup Design for Linear Systems with Imprecise Knowledge of the Actuator Input-Output Characteristics*, Springer Science and Business Media LLC, 2007.

Subchan Subchan received his Bachelor degree in mathematics from Institut Teknologi Sepuluh Nopember, Indonesia, in 1994 and a Master degree in mathematics from the Delft University of Technology, The Netherlands, in 2000. He received a Doctoral degree from the Department of Aerospace, Power, and Sensors, Cranfield University, Defence Academy of the United Kingdom, in 2006. He is currently head of the Mathematics Department, Institut Teknologi Sepuluh Nopember, Indonesia. He was vice-rector on academic affairs at Kalimantan Institute of Technology 2014-2019. He has authored a book Computational Optimal Control: Tools and Practice and published over 33 papers in peer-reviewed international and national journals and proceedings. His current research interests include system theory, dynamic modeling, optimization, and model predictive control.

Zuhair Zuhair received his Bachelor degree in mathematics from Institut Teknologi Sepuluh Nopember, Indonesia. He is currently a research assistant in the Department of Mathematics, Institut Teknologi Sepuluh Nopember, Indonesia. His current research interests include networked control systems, wireless sensor networks, control theory.

Tahiyatul Asfihani received her Bachelor, Master, and Doctoral degrees from Institut Teknologi Sepuluh Nopember, Indonesia. She is a member of the Modeling and Simulation Laboratory in the Mathematics Department, Institut Teknologi Sepuluh Nopember, Indonesia. Her current research interests include system theory, dynamic modeling, optimization, and model predictive control.

Dieky Adzkiya received his B.Sc. degree in September 2005 and an M.Sc. degree in October 2008, both in mathematics from the Institut Teknologi Sepuluh Nopember, Surabaya, Indonesia. He received a Ph.D. degree in systems and control in October 2014 and after that, he continued as a postdoctoral researcher until June 2015, both at the Delft Center for Systems and Control, Delft University of Technology, Delft, The Netherlands. Currently, he is an assistant professor in the Department of Mathematics at Institut Teknologi Sepuluh Nopember, Surabaya, Indonesia. His research interests are in the analysis and verification of max-plus-linear systems and their applications.

Seungkeun Kim received his B.Sc. degree in mechanical and aerospace engineering from Seoul National University (SNU), Seoul, Korea, in 2002, and a Ph.D. degree from SNU in 2008. He is currently a professor at the Department of Aerospace Engineering, Chungnam National University, Korea. He was an associate professor and an assistant professor at the same university from 2012 to 2020. Previously, he was a research fellow and a lecturer at Cranfield University, United Kingdom from 2008 to 2012. He is interested in micro aerospace systems, aircraft guidance and control, estimation, sensor fusion, fault diagnosis, fault-tolerant control, and decision-making for autonomous systems.